Front. Phys. China, 2007, 2(4): 410—423
DOI 10.1007/s11467-007-0054-z

REVIEW ARTICLE

LOU Qi-hong, ZHOU Jun

High power fiber lasers

Abstract In this review article, the development of the double cladding optical fiber for high power fiber lasers is reviewed. The main technology for high power fiber lasers, including laser diode beam shaping, fiber laser pumping techniques, and amplification systems, are discussed in detail. 1050 W CW output and 133 W pulsed output are obtained in Shanghai Institute of Optics and Fine Mechanics, China. Finally, the applications of fiber lasers in industry are also reviewed.

Keywords fiber laser, diode pumped laser, laser applications

PACS numbers 42.55.Wd, 42.55.-f, 42.62.Cf

1 Introduction of optical fibers

The phenomenon of total internal reflection, responsible for the guiding of light in optical fibers, has been well known two hundreds years ago [1]. Although glass fibers were made in the 1920s [2], they came into practical use only in the 1950s, when the use of a cladding layer led to considerable improvement in their guiding characteristics. Before 1970, optical fibers were used mainly for medical imaging over short distances. Their use for communication purposes was considered impractical at that time because of high losses (~1000 dB/km). However, the situation changed drastically in 1970 when, following an earlier suggestion [3], the loss of optical fibers was reduced to about 20 dB/km. Nowadays, the loss of optical fibers is only 0.1 dB/km near the 1.55 μm spectral region. The availability of low-loss fibers led to a revolution in the field of optical fiber communications.

The fiber laser has a history almost as long as that of the laser itself. Since its invention in 1963 by Elias Snitzer, the fiber laser required almost two decades of development before the first commercial devices appeared on the market in the late 1980s. These lasers used single-mode diode pumping, emitted a few tens of milliwatts, and attracted users because of their large gains and the feasibility of single-mode continuous-wave (CW) lasing for many transitions of rare-earth ions not achievable in the more-usual crystal-laser version. The most well-known application of fiber-laser technology is in 1550-nm erbium-doped fiber amplifiers [4].

For many laser applications, however, watts of optical power rather than milliwatts are required. The jump to watt-level fiber-laser output occurred in 1990, when a 4-W erbium-doped fiber laser was reported. This development laid the groundwork for ten-watt and higher single-mode fiber lasers suitable for micromachining and other applications.

Output powers of more than 1 kW have been achieved for diode pumped systems in the CW operation with diffraction-limited beam quality based on solid core rare-earth doped, low-numerical aperture, large-mode-area (LMA) fibers. The capability of fiber systems for extracting as high as several millijoules of pulse energies at ns-pulse durations has been demonstrated most recently in Yb-doped fibers. Additional sufficient pulse stretching in the time domain using the chirped pulse amplification technique is able to reduce nonlinear pulse distortions in the fiber and to extract energies in the order to limit the saturation fluence of rare-earth doped fibers even in the ultrashort pulse operation.

A further power scaling of fiber lasers and amplifiers is possible by using novel highly doped air-clad photonic crystal fibers with increased mode field diameters of the active core. This novel class of optical fibers is based on a wavelength-scale morphological microstructure along fibers, resulting in attractive guiding properties compared to conventional solid core fibers. For such an air-micro-structured

LOU Qi-hong (✉), ZHOU Jun
Shanghai Institute of Optics and Fine Mechanics, Shanghai 201800, China
E-mail: qhlou@mail.shcnc.ac.cn

Received June 20, 2007

single-mode fiber with a mode-field diameter of 35 μm, a diffraction-limited output power in the air-cooled operation of more than 3 kW can be determined, which is limited by optical damage, thermal load and nonlinearity. Water-cooling of air-micro-structured fibers will allow for output powers up to 10 kW from a single fiber. Even in the ultrashort pulse operation, pulse energies of more than 200 μJ at a repetition rate of up to 1 MHz are accessible. These parameters will allow for novel and real world applications of lasers in science and technology.

1.1 Reflection of light in optical fibers

Generally, an optical fiber consists of a core surrounded by a lower refractive index cladding, at the core-cladding interfaces of step-index fibers, and the refracted angle θ_r of the ray for an incident angle θ_i is given by

$$n_0 \sin\theta_i = n_1 \sin\theta_r \tag{1}$$

where n_0 and n_1 are the refractive indices of the fiber core and cladding, respectively. For angles larger than a critical angle ϕ_c, they are defined by

$$\sin\phi_c = n_1 / n_0 \tag{2}$$

where the rays experience total internal reflection at the core-cladding interface. Since such reflections occur throughout the fiber length, all rays $\phi > \phi_c$ remain confined to the fiber core. This is the basic mechanism behind the light confinement in optical fibers.

The maximum angle that the incident ray should make with the fiber axis to remain confined inside the core is obtain from Eq. (2)

$$n_0 \sin\theta_i = (n_1^2 - n_2^2)^{1/2} \tag{3}$$

It is called the numerical aperture (*NA*) of the fiber, which represents the light-gathering capacity of an optical fiber. For $n_1 \sim n_2$, the *NA* can be approximated by

$$NA = n_1[2(n_1 - n_2)/n_1]^{1/2} \tag{4}$$

When the optical fiber is curved, the reflective angle ϕ of an optical ray from the core boundary will be changed to $\phi = \phi \pm 1/\varsigma$, where ς is the radius of curvature. The guidance condition $\phi < \phi_c$ cannot be satisfied any more. The rays with refractive angles larger than the critical angle will be leaked outside the fiber and be lost to the optical field. Because this loss comes from the bend of optical fibers, it is named as bending loss. Other operations, such as strain, the temperature gradient and the magnetic field, can also introduce losses into optical fibers. These loss mechanisms provide opportunities to manage the propagation characteristics of optical fibers.

The dispersion effects can be explained on the basis of the behavior of the group velocity of guided modes in the optical fiber. Group velocity is the velocity at which the energy in a particular mode travels along the fiber. The group velocity is given by

$$v_g = \frac{d\omega}{d\beta} = \frac{d\lambda}{d\beta}\frac{d\omega}{d\lambda} \tag{5}$$

Thus, the group velocity is different from the phase velocity in an optical fiber.

The signal loss is defined as the ratio of optical input power (p_i) to optical output power (p_o). Optical input power is the power injected into the fiber from an optical source. Optical output power is the power received at the fiber end or optical detector. The following equation defines signal attenuation as a unit of length

$$\text{Loss} = \frac{10}{L}\lg\frac{p_i}{p_o} \tag{6}$$

Signal attenuation or loss is a log relationship. Length (L) is expressed in kilometers. Therefore, the unit of attenuation is decibels/kilometer (dB/km).

1.2 Numerical aperture of optical fibers

Figure 1 depicts a section of a clad cylindrical fiber showing the core with the refractive index of n_1 and the cladding index of n_2. Also shown is a light ray entering the end of the fiber at angle θ, reflected from the interface down the fiber. However, if angle θ becomes too great, the light will not be reflected at the interface as we described in the previous section. This angle θ is the critical angle. The *NA* is a universal description of the angle of light propagation. For example, the *NA* of a light source is given by

$$NA = \sin\alpha \tag{7}$$

where α is the project angle of the light source. The brightness of the light source is inversely proportional to the *NA* of the light source. The light from a source with an *NA* can be collected totally by an optical fiber with the *NA* larger than that of the light source. It is noticed that the capacity of an optical fiber collecting light is determined by the product of the *NA* and the fiber diameter, not the *NA* itself only.

A lens or a focal system can also have the *NA*. The *F* number equivalent to the *NA* of a lens is calculated as follows:

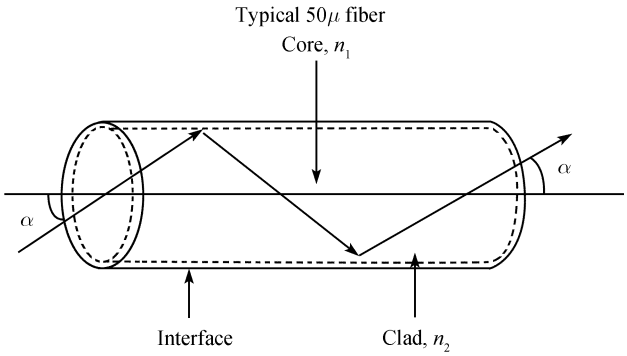

Fig. 1 Numerical aperture of an optical fiber.

$$F \text{ number} = \frac{1}{2NA} \tag{8}$$

1.3 Propagation in optical fibers

Electromagnetic field propagation in optical fibers is governed by Maxwell's equation. For a non-conducting medium without free charges, these equations provide a general wave equation for wave propagation in optical fibers

$$\nabla \times \nabla \times E = -\frac{1}{c^2}\frac{\partial^2 E}{\partial t^2} - \mu_0 \frac{\partial^2 P}{\partial t^2} \tag{9}$$

where the speed of light in vacuum is defined as usual by $c = (\mu_0 \varepsilon_0)^{-1/2}$. The solution of the wave equation that satisfies the appropriate boundary conditions and has the property that its spatial distribution does not change with propagation is called fiber modes. The fiber modes can be classified as guided modes, leaky modes, and radiation modes.

The total number of guided modes in an optical fiber is governed by the normalized frequency or simply the V parameter

$$V = k_0 a (n_1^2 - n_2^2)^{1/2} < u_m \tag{10}$$

where u_m is the mth root of the first order Bessel functions $J_m(u)$. The first root is 2.405. When an optical fiber is designed with

$$0 < V < 2.405 \tag{11}$$

the optical fiber supports only the fundamental HE11 mode. This is the single-mode condition. Otherwise, the optical fiber will support a number of guided modes and be a multi-mode (MM) fiber.

The general spatial distribution of the optical field in fibers is in the form

$$E_z = J_m(k_x^2 \rho)\, \mathrm{e}^{\mathrm{i}m\phi}\, \mathrm{e}^{\mathrm{i}\beta z} \tag{12}$$

The propagation constants β and k_x satisfy the relationship

$$k_x^2 = n_1^2 k_0^2 - \beta^2 \tag{13}$$

Obviously, the field distribution in optical fibers is different from that of the free-space beam. However, the fundamental mode in optical fibers is often approximated by a Gaussian distribution with an effective field size or usually referred to as the *spot size*:

$$E_z = A\, \mathrm{e}^{-\rho^2/w^2}\, \mathrm{e}^{\mathrm{i}\beta z} \tag{14}$$

It is noticed that the approximation to a Gaussian distribution is only valid for the fundamental mode. High order modes can not be described by a high order Gaussian beam in most cases.

1.4 Double clad fibers

Fibers widely used in the telecommunication are single-mode fibers, which consist of one cladding and one core. The core diameter of single-mode fibers is limited by the single-mode condition [see Eq. (10)], usually 5–10 μm. For the applications of communications, the fiber core can transport up to giga-byte signals over a distance of hundreds of kilometers. However, for the applications of high power fiber lasers, the core diameter is too small to carry more pump power.

To enhance the pump power capacity of single-mode fibers, double clad fibers are constructed. As their name shows, the double clad fiber consists of two cladding. The inner cladding is the multi-mode waveguide, used to contain much more pump power while the core still satisfies the single-mode condition to supply the single-mode laser output. The refractive index profile of a double clad fiber is shown in Fig. 2. The refractive indices of fiber cores are larger than those of inner claddings, which in the meantime are larger than those of outer claddings. In contrast to the fiber core of 5–10 μm with the NA of ~0.1, the inner cladding usually is $\sim n \times 100$ μm with the NA of ~0.4. The pump power capacity of double clad fibers is increased by hundreds of times higher than common single-mode fibers.

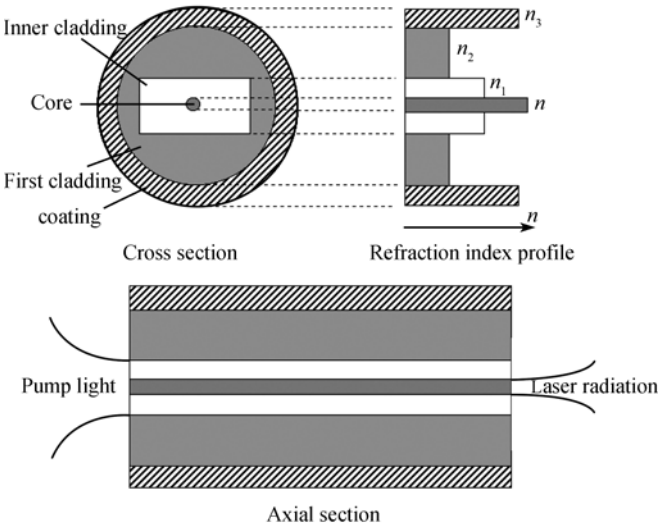

Fig. 2 Double clad fiber.

In a circular inner cladding, optical rays are reflected from the cladding boundary with a cylindrical symmetry. Most of them are trapped in the neighborhood of the cladding boundary and cannot pass through the doped core. In such a way, the pump absorption is poor. Destroying this symmetry will increase the absorption efficiency. Several types of inner claddings, e.g., D-type, rectangle, triangle, hexagonal and other irregular shapes, are proposed. In practice, D-type and rectangular inner claddings are widely used. A D-type inner cladding with the same diameter as the circular inner cladding can improve the pump absorption more than twice.

The pump absorption in a double clad fiber in the first

approximation can be given by

$$P(z) = P_0 \exp\left(-\eta\alpha \frac{S_O}{S_I} z \right) \quad (15)$$

where S_I and S_O are the cross-sectional area of the inner cladding and the fiber core, respectively. α is the absorption coefficient in the bulk material which is used to fabricate the fiber core and η is a coefficient determined by the shape of the inner cladding. The absorption coefficient is proportional to the ratio of the cross-sectional area between the inner cladding and the fiber core. The thicker the inner cladding is, the lower the absorption coefficient is.

The double clad fiber design has become standard because the large inner cladding can efficiently collect pump light, while the smaller core concentrates laser power in a smaller volume for a higher-quality output beam. The geometry of the inner cladding is chosen for efficient pumping of the core. Similar structures are used in pulsed and continuous-wave lasers. In practice, the fiber is coiled in one or more loops. Details of the design depend on the applications and power requirements.

2 Fabrication and materials

2.1 Fabrication of optical fibers

How to fabricate low loss fibers is a long-history but still interesting topic. Conversional optical fibers are made by drawing a preform which has a structure similar to that of the required fibers. There is a variety of methods for preparing preforms. They are MCVD (modified chemical vapor deposition), OVD (outside vapor deposition), VAD (vapour axial deposition), etc. The most popular method is MCVD.

In the fabrication of MCVD, a silica film is deposited on the inside surface of a fused silica tube. This tube is put on a glass working lathe and rotated. Raw halide material vapors carried by oxygen gas are introduced into it by the constant speed. The flame heats the tube from the outside to about 1600 °C. It is moved repeatedly along the tube, and during each traverse, the halide vapors are oxidized to fine glass particles and deposited on the inner surface of the tube. The heated zone can be kept at a constant temperature by controlling the flow rates of oxygen and hydrogen. The raw materials used for high silica glass are silicon, germanium and boron chlorides and phosphorus chlorate. To reduce the refractive index to be lower than that of silica, dopants such as $SiCl_4$ or BCl_3 are used; for higher values, $GeCl_4$ or $POCl_3$ are used. The flow rate is controlled by a gas supply system and the mixing ratio of halide vapors is controlled to a programmed value. By changing $GeCl_4$ concentration in the vapors for each traverse, the refractive index of each glass layer can be controlled. The metal halides (except BCl_4) remain in the liquid state at less than 50 °C given porous material. Dehydratation and consolidation follow the process. The reacted gas is exhausted from the silica tube. After sufficient film thickness is obtained, the tube is collapsed so that the deposited layers form a high index core and the tube provides a low index cladding.

Silicon dioxide, or pure silica, is usually obtained in the form of small particles (about 0.1 μm) called "soot." This soot is deposited on the target rod or tube. The depositing of the silica soot, layer upon layer, forms a homogeneous transparent cladding material. To change the value of a cladding's refractive index, some dopants are used. For example, fluorine (F) is used to decrease the cladding's refractive index in a depressed-cladding configuration.

The soot for the core material is made by mixing three gases—$SiCl_4$, $GeCl_4$, and O_2, which results in a mixture of SiO_2 and GeO_2. The degree of doping is controlled by simply changing the amount of $GeCl_4$ gas added to the mixture. The same principle is used for doping other materials.

The fabrication procedure of double clad fibers is similar to that of single clad fibers. The difference only lies in preparing the prefrom. The double clad preform is fabricated by introducing impurities into thin layers of glass tubes so that the refractive index in the preform resembles a set of concentric rings, which shows a programmed value as the double clad fibers.

Preparing a preform with pure silica free from OH^- hydroxyl ion is important to obtain low loss optical fibers. Using additional processes to remove residual OH^- hydroxyl ion from prepared perform, scientists can draw the fiber with attenuation lower than 0.1 dB/km.

2.2 Materials

Commercial optical fibers are manufactured mainly by glass or plastic. Silica glass is the most important material in the manufacture of telecommunication optical fibers. More than 95 % telecommunication optical fibers are fabricated by silica glass.

The silica system is a mixture of silicon dioxide, SiO_2 and other metal oxides, to establish a difference in the refractive index between the core and the cladding. Various dopants have been used to increase the refractive index of silica including titanium, aluminium, germanium, and phosphorus oxides.

Silica glass has excellent thermal properties with an extremely low coefficient of expansion 0.55×106 cm/°C (0–300 °C). Another related property is its high resistance to thermal shock. Thin sections can be heated and cooled rapidly without cracking. Some technical references report that the material is heated to 1100 °C, and then plunged into cold water without adverse effects.

In silica glass, the wavelengths of the operation range from 700 to 1600 nm. The wavelength of the operation is between two intrinsic absorption regions. The first region is the ultraviolet region (wavelength below 400 nm). The second region is the infrared region (wavelength above 2 000

nm). The main cause of intrinsic absorption in the infrared region is the characteristic vibration frequency of atomic bonds. Meanwhile, intrinsic absorption in the ultraviolet region is caused by electronic absorption bands.

Chalcogenide glass has a longer cut-off wavelength than oxide and fluride glass. They are solid solutions of metal sulphides, selemides and tellunides of arsenic, germanium and antimony. Chalcogenide glass is melted directly in quartz ampoules using chemically purified through distillation/sublimation. Typical melting temperature ranges from 600 °C to 900 °C. They have a stable vitreous state and a wide range of transmission wavelengths.

Fluoride glass is made from beryllium, ziroconium, mercury, aluminium and barium fluorides. They are promising materials used in the infrared wavelength range because they have very low losses in this region, up to 2 μm, whereas losses in oxide glass are comparatively high.

Phosphate glass is made from P_2O_5, SiO_2 and GeO_2, B_2O_3, Al_2O_3, and other alkali metal oxides. Phosphate glass is almost same as silica glass, in which some of SiO_2 has been replaced with P_2O_5. It has a low melting point and is transparent over a wide range of wavelengths. It has a high index of refraction and the ability to bend light at high angles.

Fluorozirconate glass comprises pre-selected molar proportions of ZrF_4, ThF_4 and BaF_2 that are essentially free of hydroxide and oxide impurities. Fluorozirconate glass produces adsorption bands at a wavelength of 2.9 μm, and casting from a melt in the presence of a mixture of He and CCl_4 in order to thereby compensate for fluorine deficiencies, which causes a formation of the color-center of Fluorozirconate glass, by the introduction of a chlorine dopant. Fluorozirconate glass is continuously transparent to light from the near ultraviolet through the near infrared spectrum substantially.

ZBLAN (zirconium, barium, lanthanium, sodium) glass is a standard fluozirconate glass system composition (ZrF_4-BaF_2-LaF_3-AlF_3-NaF). It is one of many fluoride glass compositions used to make fluoride glass and fibers. It is the most promising of these materials since its fiber-drawing region lies on the edge, or possibly just outside its crystallization region. The ZBLAN fluoride fiber is a more specific composition that uses zirconium. By varying the composition, certain optical or mechanical properties of the fiber can be optimized depending on the end user requirements.

2.3 Rare-earth doped fibers

Optical fibers play an important role in transferring optical signals, and they also act as the host medium in fiber lasers and amplifiers when the rare-earth are doped into the fiber core. Neodymium (Nd^{3+}) and Erbium (Er^{3+}) are the most common rare earth used as dopants. Other ions like Ce^{3+}, Pr^{3+}, Tb^{3+}, Dy^{3+}, HO^{3+}, Tm^{3+} and Yb^{3+} can be used in host materials like heavy metal fluoride glass fibers (ZBLAN, ZBLANPb, ZBLAB P). All these fibers can be fabricated by the vapor phase deposition of rare earth at high pressure, or by the impregnation and diffusion of rare earth doped solutions followed by drying. Generally, the concentration of rare earth materials is less than that of the classical dopants [(300–1000)$\times 10^{-6}$] for the highest gain.

The most common rare earth dopant in silica glass fibers is Yb^{3+}. The relevant energy level diagram of Yb^{3+} is very simple and consists of the $^2F_{7/2}$ ground state and $^2F_{5/2}$ excited state manifolds separated by about 10 000 cm^{-1}. The laser wavelength is around 1.05–1.1 μm in silica glass. The emission spectrum for 1000×10^{-6} Yb^{3+} doping concentration silica glass sample is shown in Fig. 3. The laser transition is $^2F_{5/2}$ to $^2F_{7/2}$ with the terminal level of 623 cm^{-1} above the ground state. The thermal energy at room temperature is 200 cm^{-1}, therefore the terminal state is thermally populated which makes Yb^{3+} a quasi-three-level system. By comparison, the terminal laser level in Nd^{3+} is about 2000 cm^{-1} above the ground state. Being a quasi-three-level system, the fiber should be pumped intensely to overcome the re-absorption. At room temperature, the thermal population of the lower laser is about 5 %. The absorbed pump power per volume needed to achieve and maintain transparency at the laser wavelength is $I = f_a n_t h\nu_p / \tau_f$, where f_a is the fraction of the total ion density n_t occupying the lower laser level; $h\nu_p$ is the energy per pump photon, and τ_f is the lifetime of the upper level. With $f_a = 0.055, n_t = 1.38\times 10^{20}\,cm^{-3}$ at 1 000 ppm doping, $h\nu_p = 2.11\times 10^{-9}$ J and $\tau_f = 0.95$ ms, the absorbed pump power needed to reach inversion is 1.7 kW/cm^3. Of course, a higher power density is required to overcome optical losses and reach laser thresholds, and for an efficient operation, the laser has to be pumped about 5–6 times above thresholds. Typically, in this laser, small volumes of material are pumped on the order of 10 kW/cm^3. Optical fibers with small cores and long lengths are suitable for Yb^{3+} laser emission. Yb^{3+} laser performance is strongly dependent on the temperature and the excellent cooling characteristics of optical fiber lasers can reduce the thermal degradation and increase the conversion efficiency.

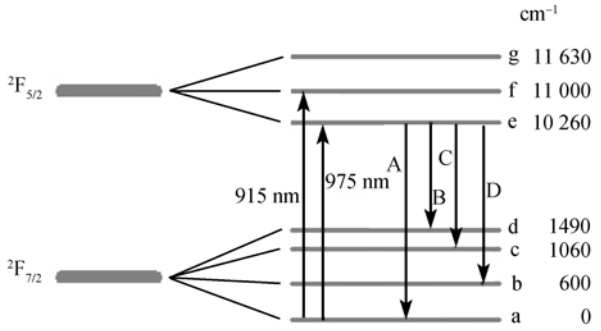

Fig. 3 Energy-level structure of Yb^{3+} in fiber.

Pumping of Yb-doped glass fibers around 915, 945 or

975 nm produces the smallest amount of heating compared to any other major laser system. Actually, the pump radiation in this material generates only about one-third of the heat compared to the Nd-doped glass laser. The fractional thermal loading is around 11 % for the Yb-doped glass laser pumped at 945 nm and 32 % for the Nd-doped glass laser pumped at 808 nm. This substantially reduced thermal dissipation is the result of a very small energy difference between the photons of the pump and laser radiation. This quantum defect or Stokes shift, is 9 % in Yb-doped glass versus 24 % in Nd-doped glass. The thermal load generated in a laser medium is of primacy concern for high-power applications. The reduced thermal heat load can potentially lead to higher-average-power systems with better beam quality than possible with Nd-doped material. Figure 4 shows the fluorescence spectrum of Yb-doped fiber DCYDF-400, and the corresponding characteristics of china made double cladding fibers are shown in Table 1.

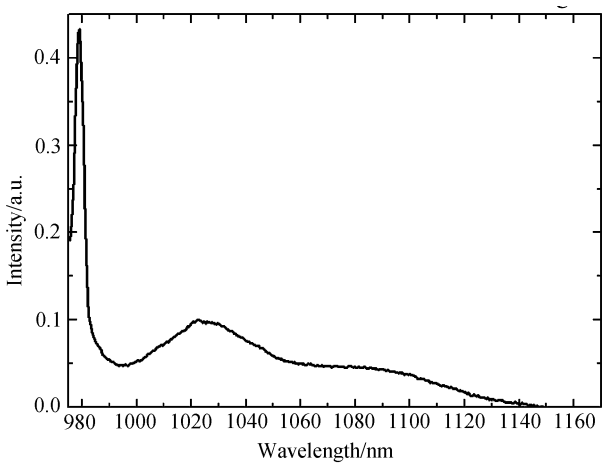

Fig. 4 Fluorescence spectrum of Yb-doped fiber DCYDF-400.

Table 1 Characteristics of two types of china made double cladding fibers.

Characteristics/types	DCYDF-400	DCYDF-650
Yb-concentration	6000×10^{-6}	6000×10^{-6}
Core diameter	8–30 μm	25–50 μm
Core NA	0.06–0.20	0.07–0.15
Geometry	D	D
Inner cladding diameter	400 μm	650 μm
Inner cladding thickness	350 μm	600 μm
Cladding numerical aperture	0.38, 0.46	0.46
Slope efficiency	> 75 %	> 75 %

3 High power lasers based on rare-earth doped fibers

3.1 Principle

Rare-earth doped silica fibers have proven to be an excellent solution for the all-optical network and have been extensively and reliably employed in the telecom arena for many years. Silica fibers are also attractive to high power amplifiers and lasers. Silica-based glass has high damage thresholds. The surface-to-volume ratio of an optical fiber is high so that heat dissipation is straightforward, and the gain medium is incorporated in a waveguide so it is possible to maintain single-mode wave propagation. Fiber manufacturing technology makes it straightforward to fabricate long fibers, and fiber laser cavities can be tailored to provide the quality beam for almost any application. Recently, there have been significant developments in the area of cladding-pumped double-clad doped-fibers for very high power fiber lasers and amplifiers. In this approach, the fiber core is heavily doped with active ions (e.g., Yb, Er, Nd, Tm) and the silica-clad fiber is coated with low refractive index materials; pump light is launched into the cladding of the optical fiber (typically in the range 125 to 650 μm in diameter). The silica inner cladding and the low index coating give rise to a high numerical-aperture multi-mode waveguide for pump light, requiring high-power multi-mode semiconductor diode lasers be used. This offers advantages both in terms of cost-per-Watt, and of the availability of more high-power high-brightness pump lasers.

In operations, the pump light propagates in the undoped cladding of the optical fiber and is absorbed by the active ions in the core. The pump power into the inner clad can be expressed as

$$P \approx 4BD^2NA^2 \tag{16}$$

where D^2 and NA are the area and numerical aperture of the inner cladding, respectively; B is the brightness of the pump source. To increase the maximum pump power coupled into the fiber, the inner cladding is designed with a high NA and a large area (typically in the range of 350 to 650 μm). From Eq. (16), in order to realize high-power output for a certain double-clad fiber, the most import thing is to have a high brightness pump source.

The pump absorption efficiency changes with the inner cladding shape. The inner cladding shape is normally non-circular to make more pump power enter the fiber core; if the inner cladding is designed to be circular, then only few pump modes cross the doped core. In this case, the pump efficiency is low. However, the core can be offset from the center or the inner cladding can be designed to be no-circular to improve the absorption efficiency. To optimize the pump absorption, various shapes of the inner cladding have been proposed. The most common shapes are described in Fig. 5.

We have calculated the absorption characteristics of double-clad fibers with circular, offset, D shaped and the unstable cavity type of inner claddings [5].

The absorption characteristics are simulated for double-clad fibers with (a), (b), (g) and (h) inner cladding shapes by the 2-D ray tracing method. The absorption efficiency of pump light is 10 %, 50 %, 80 % and 98 %, correspondingly. The results are shown in Fig. 6.

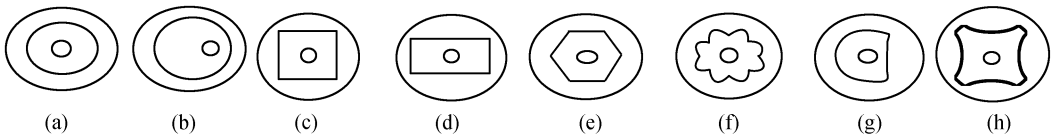

Fig. 5 Typical double clad fibers. Note: The inner cladding are **(a)** circular, **(b)** offset, **(c)** square,**(d)** rectangular, **(e)** hexagonal, **(f)** flower shaped, **(g)** D shaped, **(h)** "unstable cavity" type.

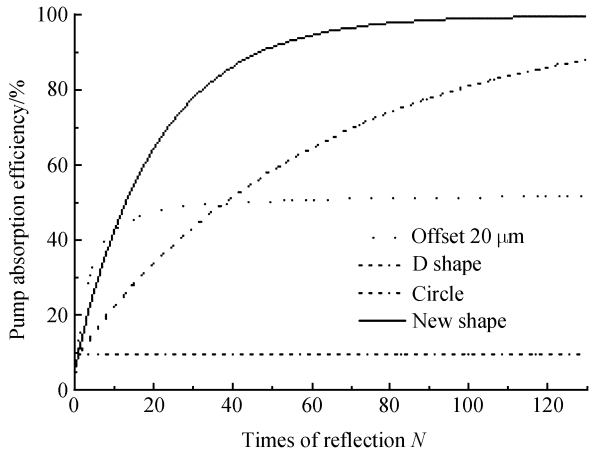

Fig. 6 Variation of absorption efficiency versus different inner shape fibers.

A fundamental limit to the power scaling of double-clad fiber lasers is the damage of the fiber core end facet in building high-power fiber lasers. In the multi-mode regime (large core), it is relatively easy to obtain a high output power, but single-mode output is a great challenge due to the optical damage. Also, onset of nonlinear processes in the fiber degrades the laser performance. Several important nonlinear processes that limit the output power and energy are stimulated Brillouin scattering (SBS), stimulated Raman scattering (SRS), and self-phase modulation. Their weights are determined by the pulse duration, spectral linewidth, and fiber length.

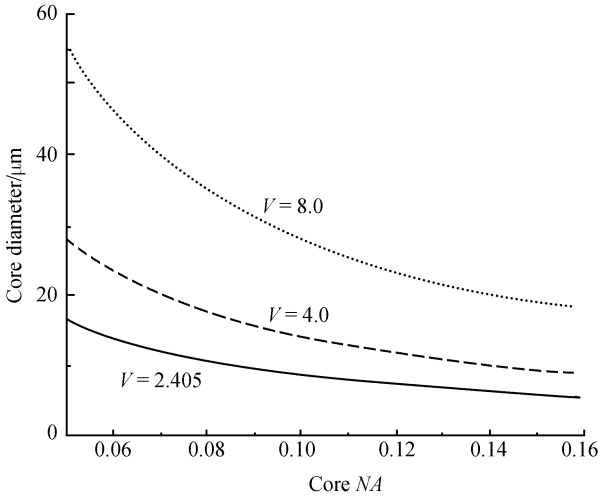

Fig. 7 Doped core diameter vs. Core *NA* (the wavelength is near 1.0 um region). Note: The size of d_{core} for the single mode fiber is less than 20 μm with an NA_{core} 0.06.

The simplest solution to overcome these problems is to increase the size of the doped core diameter d_{core}. As shown in Fig. 7, the larger d_{core} corresponds to larger V. when V >2.4, the beam quality is poor due to the propagation of higher order modes. Recently, many scientists are attempting to make use of the multi-mode power capabilities but retaining the single mode beam quality.

3.2 Laser diodes and beam shaping

The choice of the pump source is very important in the overall performance of a high-power fiber laser. It influences the reliability of cooling methods, as well as the efficiency. Historically, bulk solid state lasers have been widely used for high power applications. They can be easily pumped with lamps. But for the high-power fiber lasers, laser diodes are the best choice for the pumping. Fortunately, the development of high-power pump lasers and low-loss rare-earth doped fibers makes high power fiber lasers possible.

The difficulty in the high-brightness delivery of high-power diode laser beams stems from the geometries and structures of these devices. Thus, a high-power LDA<Author: please spell out this abbreviaton on the first mention> has a broad-area light-emitting aperture of about 1 cm × 1 μm. With such a configuration, some commercially available high power LDAs can provide 40 to 50 W of power. Much higher power can be achieved by layering high-power LDA bars in stacks.

The raw output beam from an LDA is highly divergent and suffers from two asymmetries—astigmatism and an elliptical beam profile. The divergence angles are different in two axes, the so-called "fast axis" and "slow axis". Typically, the fast axis divergence is about 40° full-width half-maximum (FWHM) while that of the slow-axis is about 10° FWHM. Sometimes the divergence can be as high as 50° × 15°.

To improve the beam quality and brightness, sophisticated beam rearrangement mechanisms are normally used. Two typical examples are the step mirror approach used by the Fraunhofer Institute for Laser Technology (Aachen, Germany) and the two-reflector approach invited by researchers in the University of Southampton (Southampton, England). Both methods have been used commercially to provide fiber-coupled laser-diode devices. A new efficient approach is developed by using groups of thin prisms for beam shaping at Shanghai Institute of Optics and Fine Mechanics (China patent No. ZL 03115584.7 by LOU Qi-hong).

3.3 End-pumping fiber laser

Coupling the pump beam into the inner cladding of the double-clad fiber through its ends by the so-called end-pumping scheme is the simplest and most efficient way to pump double-clad fibers with high-power pump sources. In the end-pumping configuration, a large inner cladding is required in order to accommodate the large pump beam of the high-power laser diode source. The laser diode pump source is either coupled to the double-clad fiber with bulk optics or fiber optics [6].

The bulk optics approach, in which the pump light is launched into the end of the fiber, is often used in laboratory applications. A major drawback is that one or both of the fiber ends are obstructed by the bulk optics used to launch the pump light. In addition, this approach lacks scalability (one fiber has only two ends) and is difficult to implement in a compact and rugged manner.

However, most updated double-clad fibers use a low-index polymer as the outer clad material to achieve the desired high numerical aperture (*NA* 0.3–0.45). These polymers have much poorer thermal stability than glass. In high-power applications, the polymer near the inner–outer clad interface can easily burn or gradually degrade during the high-power pump. Because of any faulty step in beam shaping and assembling, the high-power collimated pump beam is not so good for pumping the double-clad fiber directly. A spatial filter can be used to improve the beam quality of the high-power pump light. In order to inject the pump light into the inner cladding with high coupling efficiency, a special aspheric lens is designed and fabricated. Benefiting from the diffraction-limited performance of the aspheric lens, as well as the optical spatial filter, the focus spot and the cone angle of the pump light match well with the corresponding parameters of the double clad fiber. And the pump light can be safely and efficiently coupled into the inner cladding. The experimental setup is shown in Fig. 8. The output power is a function of fiber length when the injected pump power is fixed. The optimum length of 20 m was achieved theoretically as shown in Fig. 9. The experiment results of 6-, 21-, and 52-m fibers are presented in Fig. 10. The experimental result is in agreement with the calculated one. For one-end pumping, the maximum laser output power of 20-m DCF is more than 200 W at 1.1 μm with the slope efficiency more than 69 %; with the two-end scheme, the output power was more than 440 W [7, 8].

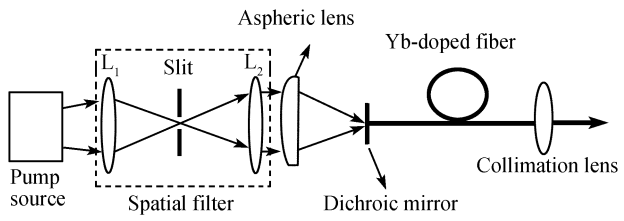

Fig. 8 Experimental setup of fiber laser with one-end-pumping using spatial filter.

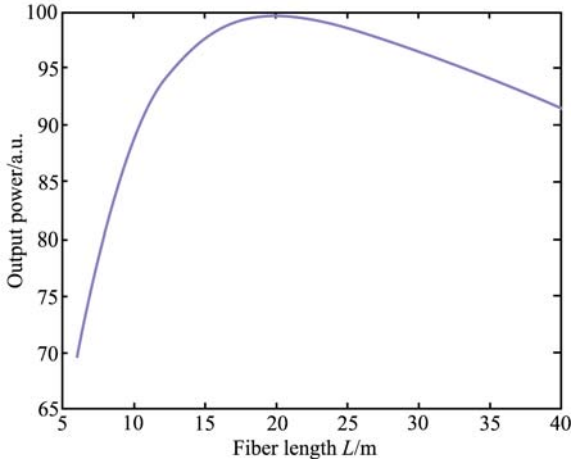

Fig. 9 Output power as a function of fiber length.

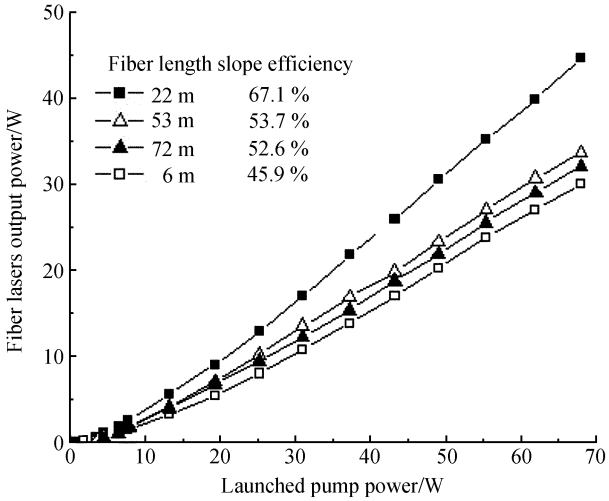

Fig. 10 Output power of different fiber lengths.

The fiber optics approach, or the so-called fused fiber bundle (pump combiner), in which several MM fibers are bundled together, fused and drawn into a taper, fusion spliced to a double-clad fiber, and then recoated with a low index polymer; pump light is launched into the double-clad fiber from individual diode lasers that are coupled to the MM fibers. Optionally, the fiber bundle can include a single-mode (SM) fiber that is used to couple signal light into or out of the core of the double-clad fiber. This method is stable and rugged and can have high coupling efficiency (ultimately limited by the efficiency of fiber-coupling of pump diodes). The approach allows unidirectional pumping and is scalable. The shape and size of the fiber bundle and of the SM pigtail must match the pumped double fiber (see Fig. 11).

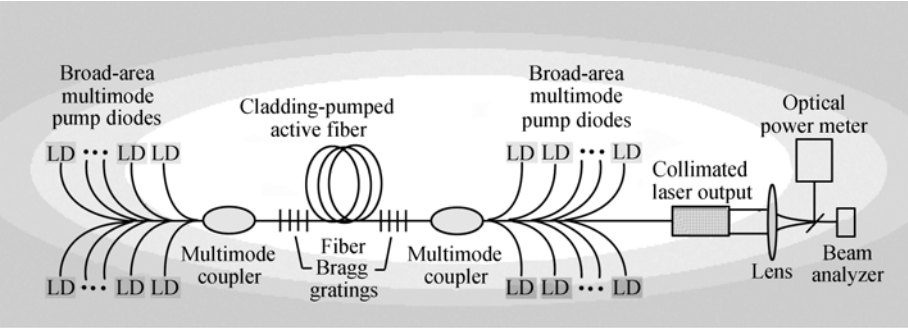

Fig. 11 Fiber laser with fused fiber bundles pumping schematic.

4 High power pulsed fiber lasers

4.1 Introduction

Recent improvements in the modified chemical vapor deposition (MCVD) process and diode-pumped lasers offer the possibility of incorporating a large variety of rare-earth ions in low-loss silica glass fibers. Interest in Er^{3+} ions was stimulated by the fact that its peak laser transition near 1.5 μm falls into the low-loss window of silica fibers. Erbium doped fiber amplifiers (EDFA) are developed rapidly and used widely in broad-band optical communication systems.

In recent years, high power pulsed fiber lasers have caused particular interest as a reliable, efficient, compact, and low cost source for a variety of applications in industry. There are several methods to obtain the pulse operation of fiber lasers. One is the Q-switch fiber laser with lower power output, and another is the master oscillator power amplifier (MOPA) system. The MOPA system is used frequently compared with CW fiber lasers. The pulse fiber laser needs higher peak power intensity on the fiber surface. Also, how to reduce amplified spontaneous emission (ASE) signal is important for the MOPA system. In this section, these problems will be discussed in detail.

In the past few years, Yb-doped fiber amplifiers have made great strides in the field of optical power amplification. Performances have been improved first thanks to new pumping technologies—end pumping has been progressively replaced by side pumping, which maks it possible to leave the double clad fiber ends free for fiber splicing. Moreover, the use of large emitting area laser diodes makes it possible to launch very high pump power, typically from a few to several tens of watts. The different shapes of the inner cladding of fibers lead to different absorption. High level saturated signal output power can thus be reached, but with reduced efficiency. This is mainly due to the fact that the shape of the cross section of the fiber and/or the transverse distribution of rare-earth ions are not optimized, leading to an inefficient absorption of the pump power.

In 2000, A Q-switched, 5 W average output power amplifier using Yb^{3+}-doped double clad fibers was reported by Alvarez-Chavez [9]. Further research was carried out by J. Limpert *et al*. at Jena, German. The single-frequency master oscillator fiber power amplifier (MOPA) emits power up to 20 W; the picosecond fiber amplifier is capable of generating 51.2 W; the nanosecond fiber amplifier can even produce up to 100 W of average power at a repetition rate of 50 kHz, corresponding to the pulse energy of 2 mJ [10–12]. In China, Lou *et al*. launched the research of high power and high energy Yb-doped double clad fibers and amplifiers at Shanghai Institute of Optics and Fine Mechanics, CAS. They used the MOPA system and the homemade large mode area (LMA) double clad fiber, realize 133.8 W of average power of amplified radiation at the wavelength of 1 064 nm and the repetition rate of 100 kHz, limited only by the available pump power. Peak power of 300 kW at 20 kHz with the pulse duration of 15 ns is obtained. Compared to the previous results with similar arrangement, it is the highest average single-fiber output power to our knowledge [7].

4.2 Transient response of Yb-doped fiber amplifier

Quasi-three-level systems such as erbium and ytterbium-doped glass fibers take part in commonly used technologies in many applications such as telecommunication devices and high-average-power systems. Because of the importance of these devices, much theoretical research has been undertaken to understand and optimize them. Two main areas have been prospected in order to characterize the behavior of fiber amplifiers. On one hand, fully numerical models allow us to predict accurately the gain and the ASE spectra, but these approaches usually take a lot of computing time and are not very suitable for a better understanding of the properties of fiber devices. On the other hand, several analytical or semi-analytical models have been developed.

The two-level rate equations neglecting ASE can be given as [9]:

$$\frac{\partial N_2}{\partial t} = (R_{\mathrm{pa}} + W_{\mathrm{sa}})N_1 - (R_{\mathrm{pe}} + W_{\mathrm{se}} + A_{21})N_2 \tag{17}$$

$$N_1 + N_2 = \rho \tag{18}$$

$$\frac{\partial P_{\mathrm{p}}^{\pm}}{\partial z} + \frac{1}{v_{\mathrm{g}}}\frac{\partial P_{\mathrm{p}}^{\pm}}{\partial t} = \pm P_{\mathrm{p}}^{\pm} \cdot \Gamma_{\mathrm{p}} \cdot (N_2\sigma_{\mathrm{pe}} - N_1\sigma_{\mathrm{pa}}) \tag{19}$$

$$\frac{\partial P_s^{\pm}}{\partial z}+\frac{1}{v_g}\frac{\partial P_s^{\pm}}{\partial t}=\pm P_s^{\pm}\cdot\Gamma_s\cdot(N_2\sigma_{se}-N_1\sigma_{sa}) \tag{20}$$

The transition rates can be described as follows:

$$R_{pa,e}=\frac{\sigma_{pa,e}\Gamma_p}{h\nu_p A_{eff}}P_p,\quad W_{sa,e}=\frac{\sigma_{sa,e}\Gamma_s}{h\nu_s A_{eff}}P_s,\quad A_{21}=\frac{1}{\tau_{21}}$$

Here, N_1 and N_2 are the population of the upper and lower status of lasers. ρ is the total density of Yb^{3+}. $\sigma_{pa,e}$ is the pump absorption and emission cross section respectively, $\sigma_{sa,e}$ is the signal absorption and emission cross section. A_{eff} is the effective core area of the YDFA and Γ_s and Γ_p give a measure of the overlap of the optical modes with the Yb distribution. τ_{21} is the fluorescence lifetime of the metastable level of the two-level system. P_p and P_s are the pump and signal power respectively. ν_p and ν_s are the pump frequency and signal frequency, and v_g is the group velocity. h is the Planck constant.

Supposing $n_i=N_i/\rho\,(i=1,2)$, the above equations can be written as

$$\frac{dn_2}{dt}=(R_{pa}+W_{sa})n_1-(R_{pe}+W_{se}+A_e)n_2 \tag{21}$$

$$n_1+n_2=1 \tag{22}$$

And we can obtain

$$\frac{dn_2}{dt}+\xi n_2=\eta$$

$$\xi=R_{pa}+W_{sa}+R_{pe}+W_{se}+A_{21},\quad \eta=R_{pa}+W_{sa}$$

The general solution is

$$n_2=ce^{-t/t_0}+\frac{\eta}{\xi},\quad c=n_2^0-\frac{n}{\xi}$$

So, the characteristic time constant

$$t_0=\frac{1}{\xi}=\tau/(1+q+p),\quad q=\frac{P_p}{P_p^{sat}},\quad P=\frac{P_s}{P_s^{sat}}$$

The initial conditions can be calculated under steady-state conditions. The pump is constant for the pumping scheme, the Gaussian signal power is 0.3 W, the duration is 1 μs, the pulse repetition rate is 20 kHz, the length of fibers is 10 m, and P_p^{sat} = 2E − 3W, P_s^{sat} = 1.5E − 2W. The finite-difference method mentioned above was used to integrate numerically with the parameters below:

$\lambda_p=915$ nm, $\lambda_s=1064$ nm, $\sigma_{pa}=2.5\times10^{-24}$ m^2

$\sigma_{pe}=3\times10^{-26}$ m^2, $\tau_{21}=0.84$ ms, $\rho=1.9\times10^{25}$ m^3

$\sigma_{sa}=3\times10^{-26}$ m^2, $\sigma_{se}=5.5\times10^{-26}$ m^2

$A_{eff}=5\times10^{-11}$ m^2

$T_p=0.001\,2$, $T_s=0.82$, $P=1000$, $q=100$

Results of computer simulation are shown above. The peak of the pulse shifts to the rising edge, which is due to the long population inversion recovery time of Yb ions. The experimental result is shown in Fig. 13, which is in agreement with the calculated results. The phenomenon demonstrates that the low repetition rate pulse has obvious transient gain. The gain saturation and recovery time depend on the pump rate.

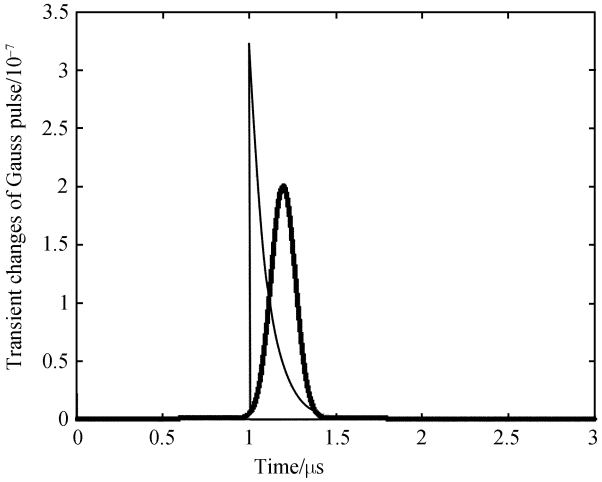

Fig. 12 Transient changes of Gauss pulse as function of time in YDFA.

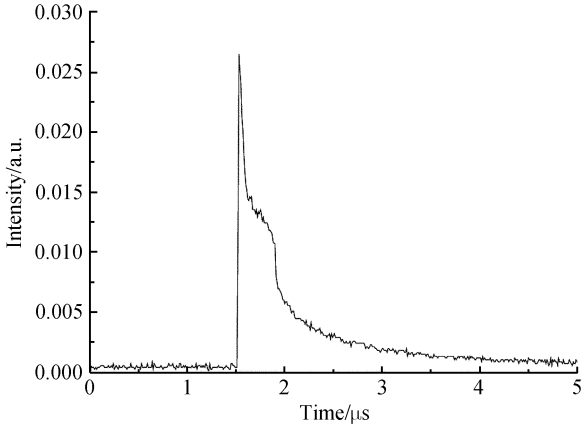

Fig. 13 Amplified pulsed profile from pulse fiber laser.

4.3 High power Yb-doped fiber amplifier

Lou *et al*. at SIOM have done much research on double-clad fiber lasers and amplifiers. They developed the 133 W fiber laser and amplifier using homemade double-clad fibers in China, which is fabricated by the Fiberhome Technology, Inc., Wuhan, China.

Increasing the size of the core appears to be one of the main directions of the technological advancement towards high energy and power, and also short length fibers are preferable as the Raman scattering can be reduced and the stimulated Raman scattering threshold can be increased.

The double-clad large-mode-area Yb-doped fibers used in

the experiment were designed by independent technology and fabricated by the standard MCVD method. The fiber has a 43 μm diameter and a Yb-doped core with an NA of 0.08, centered in the preform and a 650/600 μm D-shaped inner cladding with a NA of 0.37. The doping Yb^{3+}-concentration is evaluated to ~6500×10^{-6}.

The setup of the MOPA system is shown in Fig. 14. A Q-switched laser is applied as the seed source. The laser delivers average powers up to 1 W between the repetition rates of 20 and 100 kHz at 1064 nm. A Faraday isolator was used to protect the seed laser from back reflections. The length of the double-clad fiber is 4 m. The small cladding to core of ~200 ensures that more than 90 % of the launched pump light is absorbed in the fiber, which is coiled to a 10-cm-diameter cylindrical mandrel in the air, without any special cooling device. Polishing both fiber ends at the angles of 5°–10° suppresses laser operation and amplified spontaneous emission arising from the Fresnel reflections. The fiber amplifier is pumped by a laser diode which is water-cooled and the operating temperature from 18 to 22 °C, whose central wavelength is about 975 nm. Two lenses, which have a short focal length, are used to couple the pump light into the inner cladding with a coupling efficiency of ~90 %. A dichroic mirror with AR for pump light and HR for amplified light is placed by an angle of 45° to separate the pump light from the amplified light. Two reflective mirrors are used to shorten the length of the system. An aspheric lens is used to couple the seed light into the active core with high efficiency.

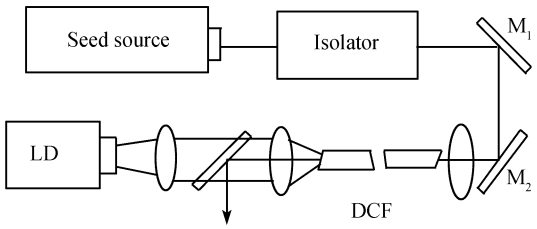

Fig. 14 Experiment setup of MOPA system.

The output characteristics are shown in Fig. 15. At a repetition rate of 100 kHz, an average output power up to 133.8 W could be produced at the maximum diode driven current. The slope efficiency with respect to the launched pump power was 56 %, and the output power increased linearly with the launched pump power. Compared to the previous results with similar arrangement, it is the highest average output power to our knowledge. No facet damage has ever been found at the maximum power. So more output power can be realized if the pump power is increased. Due to the transient gain of the MOPA system, the amplified pulse duration is reduced from 30 to 15 ns at the repetition rate of 20 kHz, corresponding to a peak power of 300 kW. The factor of pulse shortening increases with the decrease in the repetition rate. Figure 16 shows the emission spectrum at the maximum output power, against the seed source spectrum and ASE on the logarithmic scale at the repetition rate of 100 kHz. When the fiber was pumped without injection of the seed source, the output spectrum was ASE spectrum and centered at 1040 nm with a 3 dB bandwidth of 20 nm, but when the seed source was coupled into the core, the output peak spectrum was shifted to 1064 nm due to mode competition. The ASE spectrum was reduced effectively and no stimulated Raman scattering occurred. Coiling the fiber in a diameter less than 10 cm suppressed higher order transversal modes through bending losses, and only lower order modes are amplified. The M^2 value is characterized to be 3.2. This value could be improved with a cylindrical mandrel of a smaller diameter.

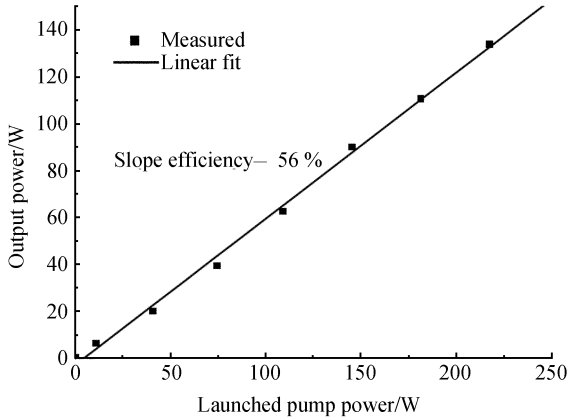

Fig. 15 Output power against launched pump power.

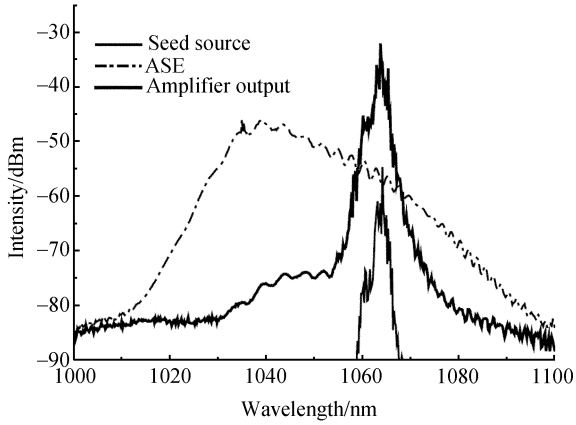

Fig. 16 Emitted spectrum of seed source, amplifier output and ASE.

The modeling and experiments presented here are not the last word on any of these subjects. There is still a great deal of work to be done to scale the fiber amplifier system to high power. Additional work must be done to improve beam quality. The variation in amplifier performance with temperature is unlikely to be a major difficulty. However, as amplifiers are scaled to kW levels, eliminating waste heat becomes a concern. Short fibers, while reducing SBS, make heat removal more difficult. A very short fiber will have some of the same thermal problems as a rod laser. In addition, elevated core temperatures may cause diffusion of the core dopants and changes in the guiding properties. A

great challenge that has not received much attention is the need for high-power and low-loss isolators. Low-loss fiber pig- tailed isolators can only operate in the hundred mW regime. High-power bulk isolators require free-space propagation. It also introduces a place subject to misalignment, negating the greatest advantage of fiber systems.

5 Recent development and applications of fiber lasers

5.1 Recent development

Fiber lasers are a technological revolution in the fields of solid state lasers: there has been a rapid, large increase in the power produced by fiber laser systems. Recently, the level of continuous wave (CW) power available in single double-clad fibers has been increased from about hundreds of Watts to more than 1 kilowatt. This breakthrough has been driven by two factors: one is the progress in the development of high brightness semiconductor diode pumping sources; the second is the use of large mode area (LMA) fibers.

The remarkable rise in CW fiber laser output powers that has been reported by several research groups over the past few years is illustrated in Fig. 17. This figure shows only the results achieved in a single double-clad fiber. An array of combined fiber lasers with an output close to 10 kW have been reported.

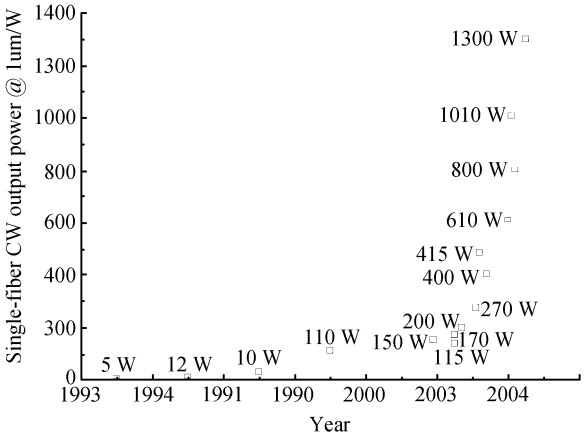

Fig. 17 Recent progress of CW laser output with single double cladding fiber.

The achievement of higher laser powers is limited by three factors: the first is the optical damage of the fiber material by high power lasers; the second is the limitation by the usable pump powers with higher brightness; and the third is the effects of nonlinear interaction on the fiber core [13].

The development of the optical fiber has traditionally been driven by the need of long distance optical communication links. During the 1970s, the trend was shifted from the large multi-mode to small single-mode core, and the intermodal dispersion is much smaller in the single-mode core compared to the multi-mode fiber core. However, the need of high CW power or high average pulse fiber lasers is pushing the double clad fibers to the opposite direction—increasing the fiber core dimensions. For standard telecommunication fibers, the core diameter is usually less than 10 μm, and the core diameter of a typical high power LMA double cladding fiber is around 30 μm. The ten-time larger core area makes the ten-time higher output power possible.

The pumping power with high brightness is another key point in developing high power fiber lasers. Recently, the high power diode laser model with a total output of more than 750 W with the centre wavelength of 975–980 nm is available. The output can be transmitted by a fiber with a core diameter of 600 μm. By using the two end pumping configuration, 1 kW of laser output can be obtained. On the other hand, several fiber pigtail diode pumps can be coupled into a double cladding fiber by using a fiber combiner. This combiner consists of several relatively large-diameter pump fibers fused together with a signal-carrying fiber, which contains a core matching that of a LMA fiber. The fused pump fibers are tapered at the end to match the dimensions of the double cladding fiber, being cleaved and then spliced to a rare-earth doped LMA fiber. With this diode-combining scheme, several low power diodes can be used instead of a single high power one. The maximum power of this kind of combining system is around 200 W.

Since the magnitude of the laser-signal distortion induced by nonlinear effects (such as stimulated Raman scattering, SRS) is inversely proportional to the fiber mode area, the LMA fiber has a mode area more than ten times larger than the standard one. Because the standard single-mode fiber at 1.064 μm typically supports a fundamental mode with a diameter of ~6.2 μm and a corresponding mode area of 30 μm^2, when the LMA fiber is used with a core diameter of 30 μm, the mode field diameter is ~24 μm with a corresponding mode area of 452 μm^2. The SRS threshold for the CW fiber laser is typically in the 100 W range and that of LMA is in the kilowatt range. For pulsed fiber lasers, the SRS threshold for standard fibers is only ~20 kW peak power, and for LMA (30 μm core), it can be increased to ~300 kW.

Although the LMA fiber has advantages described above to increase the total output power from a single double cladding fiber laser with higher SRS thresholds, the beam quality of the LMA fiber laser is decreased. Because LMA fibers with core sizes of larger than 10 μm support more than one transverse mode, it is necessary to employ some specific techniques to achieve the single-mode operation of LMA fiber lasers. For example, in a coiled fiber, higher order mode can be filtered to offset the effects of intermodal scattering. In practice, by using short-length high-quality LMA fibers, it has proved possible to obtain a nearly diffrac-

tion-limited beam output.

In contrast to all other optically pumped solid state lasers, fiber lasers use guided-mode propagation to create a new kind of laser structure with very long resonator lengths. The laser cavity is extremely simple without the need for complex alignment. What are limiting factors for scaling the power of the fiber laser in future? It is likely that within next few years, research and development efforts will continue to extend the output power with a single fiber into the several kilowatt range. Since current approaches to produce LMA fibers are close to their limits in terms of the mode area that can be achieved, to design and develop new, large mode area fibers would be highly advantageous. One new idea is the hollow core rare-earth doped photonic crystal fiber (PFC), which can reduce the nonlinearity of the fibers; another one is short centimeter-size fiber lasers with large core areas. Fiber geometry offers another promising avenue for power scaling. Several fibers can easily be packaged together, and the optical combination of the outputs of these fibers could lead to higher power than what an individual one can provide. A variety of techniques for incoherent and coherent combination of fiber lasers is now being studied and developed. Much higher power can be obtained in future.

5.2 Applications of fiber lasers

Fiber lasers have become the “hotbed of solid state laser development” with advance in powerful output, better ways to generate short pulses at high average power and higher efficiency. According to the annual market review and forecast, the LASER FOCUS WORLD started a report on fiber laser sales only a few years ago. In 2004, the total sales of fiber lasers reached $84 million; it was 14 % over 2003; additionally, a growth of 47 % was expected in 2005. The reasons for this strong growth are new technologies and ideas, including the improvement in fiber design and fabrication and steady improvement in the pump diode source.

In various applications, fiber lasers can be used in the fields of material processing, medical applications, instrument and basic research, in which, the main field is the material processing. It includes welding, cutting, drilling, marking and semiconductor or microelectronics manufacturing [14]. The requirements for the flexible tool are as follows.

(1) Good beam quality. Compared with other lasers, fiber lasers have very nice beam quality with M^2 less than 1.5 with a core diameter < 10 μm. For large core diameters, more than 600 W with M^2 < 1.2 has been demonstrated recently.

(2) Flexibility in spot geometry. The fiber laser is delivery by the double cladding itself, and no additional transmission fiber is needed.

(3) Flexibility in time. CW and pulse output are available from fiber lasers; usually, a master oscillator power amplifier scheme is used to generate pulse output.

Laser processing technology is widely used in car manufacture, areospace industry and many other fields. It is the tendency of material processing in the future and has most advanced advantages compared with other processing methods. Three-dimensional laser processing makes it possible to realize the processing of three-dimensional workpiece by the high density laser beam along the complicated special curve for welding, cutting and other treatments. The fiber laser is held by a robot arm, normally, five or six degree of freedom to reach any position of the workpiece. In this system, the focus characteristics of the fiber laser beam keep constant at different processed positions during the processing.

Laser micro-machining is another application field for fiber lasers. As microelectronic circuits continue to shrink, the use of lasers in circuit production continues to grow. Because the fiber laser can be focused to very small points, it can be used for the laser trimming of thick- and thin-film resistors on ceramic and silicon substrates and laser repair of redundant memory devices. The fiber laser is fast becoming a viable tool in a wide variety of micro-maching applications. Typical lamp pumped lasers for trimming applications required high energy input power supplies (for example 3 kW), large cooling water systems, periodic lamp and water filter replacement; it also needs frequent output power monitoring and adjustment. However, the LD pumped fiber laser requires only a few hundred watts of input power and provides constant, stable laser energy for thousands of hours. With the improved quality of nonlinear crystals, such as BBO and LBO, the process in the laser micro-machining can get smaller focal points by using the second or the third harmonic generation in the green or UV regions. It would achieve better results with much cleaner cuts and less thermal affected zones.

Laser marking is one of the most important applications for laser material processing especially in China. Fiber lasers can be used in laser marking systems with several advantages—good beam quality with almost diffraction limited beam spread angles, compact size with flexible fiber output, high plug efficiency (more than 20 %) with low operating cost and air-cooling systems. Figure 18 shows the fiber laser marking system developed by Shanghai Institute of Optics and Fine Mechanics.

Fig. 18 Laser marking system developed by SIOM.

The system can make marks in the region of 100 mm×100 mm with a scanning speed of 30 m/s. The fiber laser used in this system is a 10 W pulsed fiber with the repetition rate between 20 to 100 kHz, and the laser beam spread angle is 2 mrad.

Acknowledgements This work was supported by the National Natural Science Foundation (Grant No. 60244005), and by Shanghai Science Foundation (Grant No. 05DZ22001), and by Chinese Academy of Sciences.

References

1. Born M. and Wolf E., Principle of Optics, New York: Cambridge University Press, 1999
2. Chuang S., Physics of Optoelectronic Device, New York: John Wiley & Sons, Inc., 1995
3. Kao K.C. and Hockham G. A., Dielectric-fibre Surface Waveguides for Optical Frequencies, Proc. IEE,1966, 113: 1151
4. Millar S. and Kaminow I., eds, Optical Fiber Telecommunications–II, New York: Academic, 1988
5. Zhou J., Lou Q. H., Wang Z. J., Dong J. X., and Wei Y. R., SPIE, 2002, 4914:141
6. Dominic V., MacCormack S., Waarts R., et al., Electronics Letters, 1999, 35(14):1158
7. Lou Q. H., Zhou J., and Zhu J. Q., 133 W high-average-power pulsed fiber laser, IQEC/CLEO-PR 2005, Tokyo, Japan, Post deadline paper. No. 00989
8. Xue D., Lou Q., Zhou J., Kong L., Li J., and Li S., Chinese Optics Letters, 2005, 3(6): 345
9. Alvarez-Chavez J. A. and Offerhaus H. L., Opt. Lett, 2000, 25(1): 37
10. Hofer S. and Liem A., Opt. Lett., 2001, 26(17): 1326
11. Limpert J. and Liem A., Opt. Lett., 2001, 26(23): 1849
12. Limpert J. and Hofer S., Appl. Phys. B, 2002, 75: 477
13. Galvanauskas A., Optics & Photonics News, July 2004: 42
14. Sun Y. and Swenson E. J., SPIE, 2003, 4915: 17